Pharmaceutical Research, Vol. 10, No. 9, 1993

Research Article

Synthesis and Pharmacokinetics of a New Liver-Specific Carrier, Glycosylated Carboxymethyl-Dextran, and Its Application to Drug Targeting

Makiya Nishikawa,[1] Akiko Kamijo,[1] Takuya Fujita,[1] Yoshinobu Takakura,[1] Hitoshi Sezaki,[2] and Mitsuru Hashida[1,3]

Received September 21, 1992; accepted February 18, 1993

To develop a new carrier system for hepatic targeting, carboxymethyl-dextran (CMD) was modified with galactose and mannose residues (Gal-CMD, Man-CMD), and their disposition characteristics were studied in mice using ^{14}C-labeled dextran. At a dose of 1 mg/kg, i.v.-injected Gal-CMD and Man-CMD rapidly accumulated in the liver parenchymal and nonparenchymal cells, respectively, because of their preferential uptake via carbohydrate receptors in these cells. Pharmacokinetic analysis revealed that their uptake rates were sufficiently large for selective drug targeting. Targeting of cytosine β-D-arabinoside (araC) was studied using Gal-CMD as a specific carrier to the hepatocytes. From the conjugate of araC with Gal-CMD, araC was released with a half-life of 36 hr in phosphate buffer (pH 7.4) and 23 hr in plasma. An *in vivo* biodistribution study demonstrated a disposition profile of the conjugated araC similar to that of the carrier, and selective delivery to hepatocytes of up to 80% of the dose was achieved. These findings suggest that glycosylated CMDs are carriers with a high affinity to liver parenchymal or nonparenchymal cells without any affinity to other tissues.

KEY WORDS: drug targeting; sugar recognition; glycosylated dextran; pharmacokinetics; cytosine β-D-arabinoside.

INTRODUCTION

Carbohydrate receptors in the liver, i.e., asialoglycoprotein receptor in hepatocytes and mannose receptor in Kupffer and liver endothelial cells (1,2), have enabled the selective drug targeting to this organ (3–5). Several trials of drug targeting utilizing macromolecular carriers with sugar moieties such as asialoglycoproteins (6) or chemically glycosylated proteins (7,8), poly(amino acids) (9), and synthetic polymers (10) have been carried out. Recently, we analyzed the *in vivo* disposition of glycosylated bovine serum albumins (BSA) by a physiological pharmacokinetic model and clarified the possibility and the limitation of these glycosylated carriers in drug targeting (11). Application of these findings to proteinous drug led to the development of glycosylated superoxide dismutase (12).

The use of asialoglycoproteins or chemically glycosylated proteins as drug carriers may have some disadvantages, e.g., difficulty in drug conjugation, immunogenicity, and undesirable specific tissue interaction of the carrier proteins (13). Therefore, development of an alternative carrier backbone is strongly required. In this case, a liver-specific carrier must be designed to have adequate physicochemical properties to escape from any undesirable recognition by other tissues in addition to the introduction of carbohydrate residues as a homing device. In our series of investigations, we have systematically examined the relationship among physicochemical, pharmacodynamic, and pharmacokinetic characteristics of model macromolecules and their drug conjugates (14–18). These studies revealed that macromolecules with a relatively high molecular weight and anionic charge were retained in the circulation for a long time (18) and thus can serve as a favorable backbone for introducing a homing device onto them.

In this study, we selected dextran as a carrier backbone because of its high water solubility, abundance of hydroxyl groups applicable for chemical modification, low immunogenicity, and long experience in clinical use as a plasma expander (19). We modified dextran to the carboxymethylated form (CMD) to minimize the interaction with body components (20) and then coupled them with galactose or mannose (Gal-CMD, Man-CMD). In addition, the potential of glycosylated CMD in drug targeting was evaluated using cytosine β-D-arabinoside (araC) as a model drug.

MATERIALS AND METHODS

Chemicals

Dextrans with average molecular weights of approximately 70 kD (T-70) and 10 kD (T-10) were purchased from

[1] Department of Basic Pharmaceutics, Faculty of Pharmaceutical Sciences, Kyoto University, Sakyo-ku, Kyoto 606-01, Japan.
[2] Department of Basic Pharmaceutics, Faculty of Pharmaceutical Sciences, Setsunan University, Osaka 573-01, Japan.
[3] To whom correspondence should be addressed at Faculty of Pharmaceutical Sciences, Kyoto University, Sakyo-ku, Kyoto 606-01, Japan.

0724-8741/93/0900-1253$07.00/0

Pharmacia, Uppsala, Sweden. Bovine serum albumin (BSA; fraction V), β-D-galactose, and α-D-mannose were obtained from Nacalai Tesque, Kyoto, Japan. Collagenase (type I) was obtained from Sigma, St. Louis, MO. [5-^{3}H]Cytosine β-D-arabinoside and potassium [^{14}C]cyanide were purchased from Amersham Japan, Tokyo. Indium chloride ([^{111}In]Cl_3) was a gift from Japan Mediphysics, Tokyo. All other chemicals were reagent-grade products obtained commercially.

Radiolabeling of Dextran

[Carboxyl-^{14}C]dextran (T-70) was prepared as previously described (18). Briefly, 0.05 mmol of dextran (T-70), sodium bicarbonate, and sodium hydroxide was dissolved in 5 mL of distilled water and frozen in a glass tube. Then potassium [^{14}C]cyanide (0.05 mmol) was added and the tube was sealed in a flame. The mixture was thawed, stored at 45°C for 24 hr, and heated for 7 hr at 50°C in a stream of air to effect hydrolysis. The product was purified by gel filtration using a Sephadex G-25 (Pharmacia, Uppsala, Sweden) column and concentrated by ultrafiltration. The specific activity of dextran (T-70) was 0.025 MBq/mg.

Preparation of Dextran Derivatives

Carboxymethyl-dextran (CMD) was synthesized as previously reported (18). Glycosylation of CMD was performed as follows. Carboxymethyl-dextran (1 g) was dissolved in 30 mL of distilled water, and 1-ethyl 3-(3-dimethylaminopropyl) carbodiimide (1 g) was slowly added to the solution at pH 5.0. Then ethylenediamine (100 μl) was added and the pH of the solution was kept at 5.0 by the addition of a 1 *N* HCl solution. The reaction was allowed to proceed overnight with stirring and the solution was dialyzed against distilled water. Sugar residues were incorporated to amino groups of ethylenediamine-coupled CMD by the method of Lee *et al.* (21) using 2-imino-2-methoxyethyl 1-thiogalactoside or 1-thiomannoside, and galactosylated CMD (Gal-CMD) and mannosylated CMD (Man-CMD) were obtained (Fig. 1). Their electric charges were checked by a batch method using a CM-Sephadex C-50 cation exchanger and a DEAE-Sephadex A-50 anion exchanger (Pharmacia, Uppsala, Sweden) as described previously (18). Numbers of sugar molecules attached on dextran derivatives were determined by the anthrone-sulfuric acid method. The change in numbers of free amino groups was also determined using 2,4,6-trinitrobenzene-sulfonic acid. The apparent average molecular weights of all synthesized dextran derivatives were in the area between 80 and 100 kD determined by gel chromatography and no aggregates were observed. The size distribution of dextran derivatives was not wider than the native dextran used in this study (M_w/M_n = 1.97). Radiolabeled dextran derivatives were synthesized using ^{14}C-labeled dextran (T-70). Glycosylated CMDs synthesized from dextran (T-10) were used only in the hepatic uptake inhibition experiment for glycosylated BSAs.

Attachment of araC to Dextran Derivatives

Coupling of araC to carboxyl groups of CMD (araC-CMD) and Gal-CMD (araC-Gal-CMD) was performed through the peptide bond with condensation (22). Isobuthylchloroformate (105 μl) and triethylamine (100 μl) were added to a suspension of CMD or Gal-CMD (100 mg) in dry DMF (50 mL) at under −10°C and the mixture was stirred at this temperature for 2 hr. araC was added to the suspension and the reaction was allowed to proceed at room temperature for

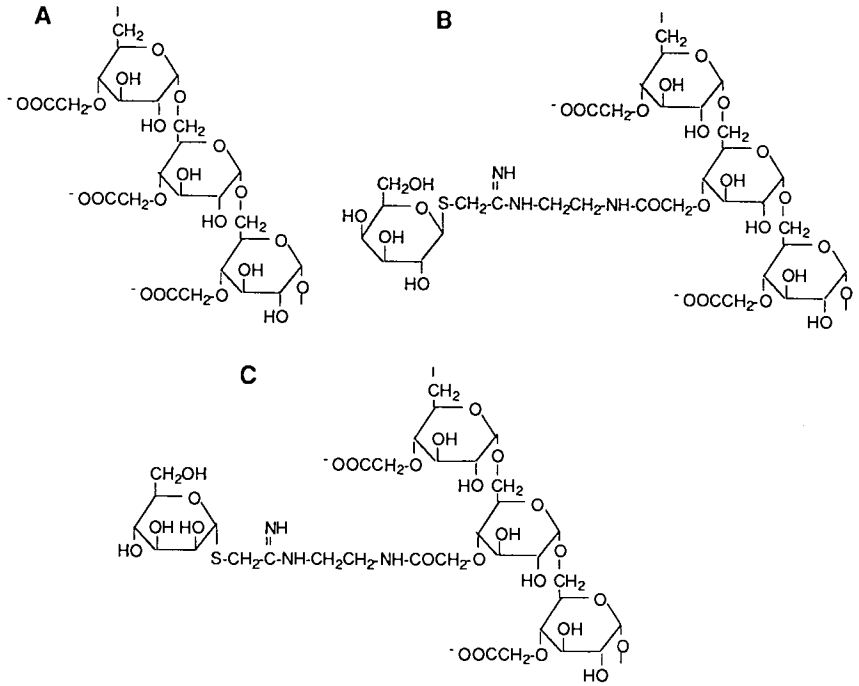

Fig. 1. Representative chemical structures of dextran derivatives. (A) Carboxymethyl-dextran (CMD); (B) galactosylated carboxymethyl-dextran (Gal-CMD); (C) mannosylated carboxymethyl-dextran (Man-CMD).

3 days. Then the reaction mixture was dialyzed against distilled water and concentrated by ultrafiltration. araC-Gal-CMD was synthesized by two methods as shown in Fig. 2. In method I, araC was coupled to previously synthesized Gal-CMD [araC-Gal-CMD (I)]. In method II, araC was coupled to CMD and then galactose residues were attached to araC-CMD [araC-Gal-CMD (II)]. The numbers of incorporated araC molecules were determined by the UV absorption at λ_{max} 300 nm. For *in vivo* experiments, the conjugates were synthesized with [^{3}H]araC as described above.

Determination of Release Rate of araC from the Conjugates

The release rate of araC from conjugates was determined in 0.1 *M* phosphate buffer (pH 5.0, 7.0, 7.4, and 8.0) at 37°C. Conjugates dissolved in buffer at different pH's were kept in a sealed cellulose tube and the tube was soaked in the same buffer. The tube was incubated at 37°C and the solution outside the tube was sampled to determine the amount of araC released at λ_{max} 272 nm (e 9000). To determine the stability in plasma, 100 μL of the buffer solution (pH 7.4) containing araC-CMD synthesized with [^{3}H]araC was added to 300 μL of mouse plasma and the solution was incubated at 37°C. The amount of araC released was measured by gel filtration (Sephadex G-25).

In Vivo Distribution Experiment

Male ddY mice (25–28 g) were obtained from the Shizuoka Agricultural Co-operative Association for Laboratory Animals, Shizuoka, Japan. Mice received a 1 mg/kg dose of ^{14}C-labeled dextran derivatives or ^{3}H-labeled araC conjugates with dextran derivatives in saline by tail vein injection and were housed in metabolic cages for urine collection. At various periods after injection, blood was collected from the vena cava under ether anesthesia and the mice were killed. The heart, lung, liver, spleen, kidney, intestine, muscle, and iliac lymph nodes were excised, rinsed with saline, weighed, and subjected to assay. Distribution of ^{14}C-labeled dextran derivatives and ^{3}H-labeled araC-dextran derivative conjugates in liver parenchymal (PC) and nonparenchymal cells (NPC) was determined in different mice by fractioning PC and NPC after collagenase perfusion. Cross-contamination of PC and NPC was less than 2% determined by microscopy.

Simultaneous Administration of Glycosylated Dextran and Albumin Derivatives

Glycosylated bovine serum albumins were synthesized and radiolabeled with ^{111}In using DTPA anhydride as reported previously (11). ^{111}In-labeled glycosylated albumin was injected at a dose of 1 mg/kg with glycosylated dextran with average molecular weights of about 10 kD at a dose of 20 mg/kg. In a similar manner, radiolabeled Man-CMD (70 kD) was coadministered with Man-BSA. At various periods after injection, plasma and liver were sampled and subjected to assay for radioactivities. Differences in radioactivity distribution were statistically evaluated by Student's *t* test.

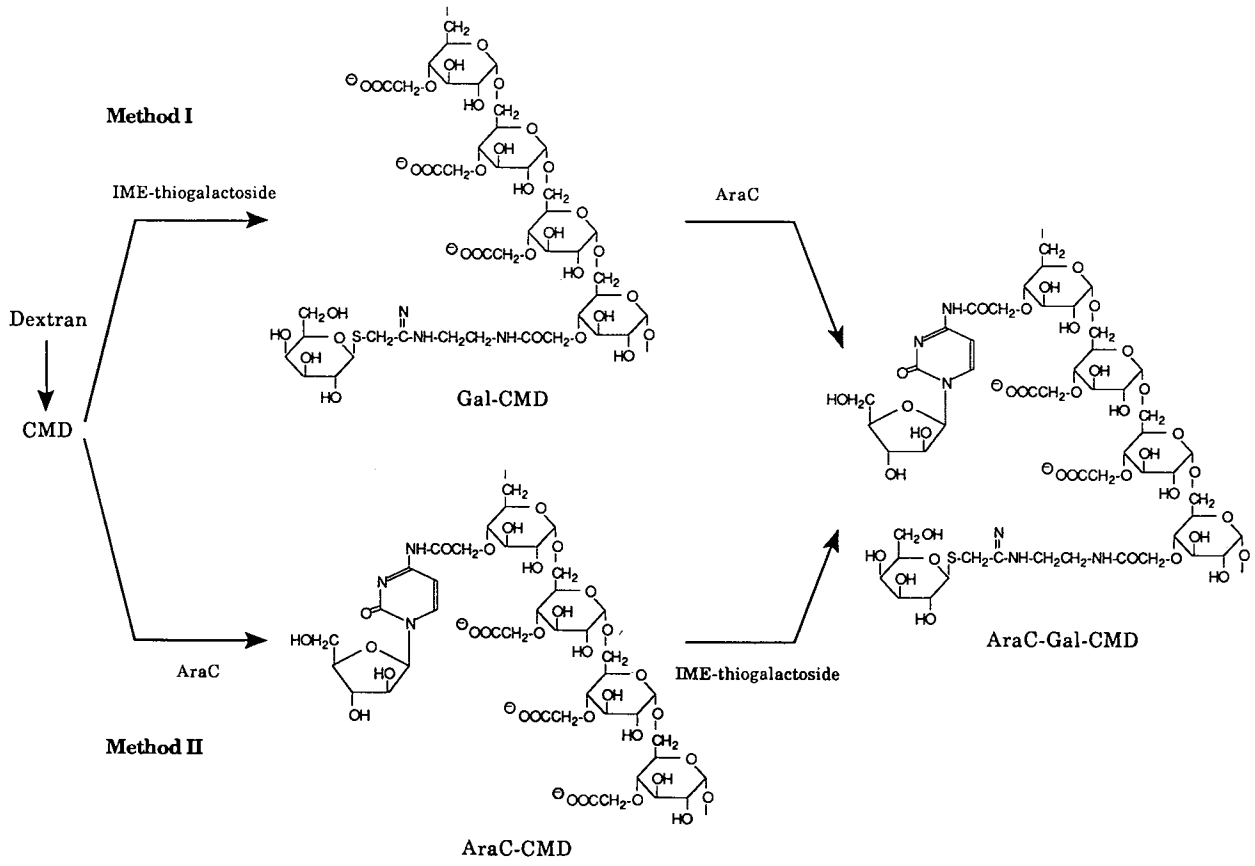

Fig. 2. Synthetic procedures of araC conjugates with carboxymethyl-dextran derivatives.

Analytical Methods

The radioactivity of ^{14}C or ^{3}H in plasma, urine, and tissues was measured using a liquid scintillation counter (LSC-5000, Beckman, Tokyo) after dissolution with Soluene-350 (Packard, Netherlands) and added with a scintillation medium Clear-sol I (Nacalai Tesque, Tokyo). The ^{111}In radioactivity was counted in a well-type NaI-scintillation counter (ARC-500, Aloka Co., Tokyo).

Data Analysis

The tissue distribution was evaluated using a tissue uptake rate index calculated in terms of clearance as reported previously (16). The change in the amount of radioactivity in the tissue with time can be described as follows:

$$dT(t)/dt = Cl_{in}C(t) - K_{out}T(t) \quad (1)$$

where $T(t)$ (% of dose/g) is the amount of radioactivity in 1 g of the tissue, $C(t)$ (% of dose/mL) is the plasma concentration of radioactivity, Cl_{in} (mL/hr/g) is the tissue uptake rate index from the plasma to the tissue, and K_{out} (1/hr) is the efflux rate constant from the tissue. In the present study, the efflux process is considered to be negligible during the time studied (see Discussion). Ignoring efflux, Eq. (1) integrates to

$$Cl_{in} = T(t1) \Big/ \int_0^{t1} C(t)dt = T(t1)/AUC_{0-t1} \quad (2)$$

According to Eq. (2), the tissue uptake rate index is calculated using the amount of radioactivity in the tissue at any time and the area under the plasma concentration–time curve (AUC) up to that time. Then the organ clearance (CL_{org}) is expressed as follows:

$$CL_{org} = Cl_{in}W \quad (3)$$

where W (g) is the total weight of the organ. We have also calculated total-body clearance (CL_{total}) from AUC for an infinite time (AUC_∞) by the following equation:

$$CL_{total} = Dose/AUC_\infty \quad (4)$$

RESULTS

Tissue Distribution and Urinary Excretion of ^{14}C-Labeled Dextran Derivatives

Figure 3 shows the plasma concentration– and liver accumulation–time curves of ^{14}C-labeled CMD, Gal-CMD, and Man-CMD after intravenous injection in mice at a dose of 1 mg/kg. The attachment of sugar moieties to CMD greatly affected the disposition property of CMD. CMD showed slower elimination from plasma and little accumulation in the liver, while Gal-CMD and Man-CMD were rapidly eliminated from the plasma and accumulated in the liver. The amounts of dextran derivatives excreted in the urine before complete removal from the blood also changed with glycosylation from 32% of the dose (CMD) to 7.3% (Gal-CMD) and 7.3% (Man-CMD). Man-CMD was also taken up by the spleen but no significant accumulation of radioactivity was observed in any other tissue for either Gal-CMD or Man-CMD.

Pharmacokinetic Analysis of the Disposition Properties of ^{14}C-Labeled Dextran Derivatives

Table I summarizes the total-body, hepatic, and urinary clearances, AUC_∞, and tissue uptake rate index for representative tissues calculated from the results shown in Fig. 3. The total-body clearance of CMD was small, reflecting its long retention in the circulation (Fig. 3). Gal-CMD and Man-CMD showed high hepatic clearance values which occupied a greater part of the total-body clearance. The uptake rate in the liver of Gal-CMD was much higher than that of Man-CMD.

Cellular Localization of ^{14}C-Labeled Dextran Derivatives in the Liver

Figure 4 shows the amount of dextran derivatives accumulated in 10^7 cells of PC and NPC at 30 min after injection, and that of the glycosylated BSAs (11) is also shown for comparison. Little CMD was recovered in the PC or NPC, which reflects its small accumulation in the liver (Fig. 3). Gal-CMD was preferentially taken up by the PC, while Man-

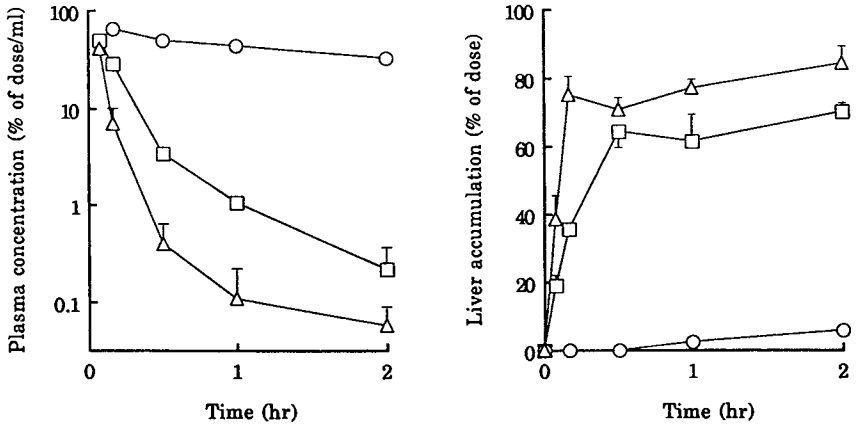

Fig. 3. Plasma concentration– and liver accumulation–time curves of ^{14}C-labeled CMD (○), Gal-CMD (△), and Man-CMD (□) after intravenous injection in mice at a dose of 1 mg/kg. Results are expressed as the mean ± SD of four mice.

Table I. AUC, Clearance, and Tissue Uptake Rate Index for ^{14}C-Labeled Dextran Derivatives After Intravenous Injection in Mice at a Dose of 1 mg/kg[a]

Compounds	AUC (% of dose hr/mL)	Clearance (μL/hr)			Tissue uptake rate index (μL/hr/g)			
		CL_{total}	CL_{liver}	CL_{urine}	Liver	Spleen	Kidney	Muscle
CMD	195	512	147	185	139	59.1	26.6	3.7
Gal-CMD	5.6	17,800	15,100	1,310	12,200	13.2	547	56.8
Man-CMD	14.4	6,930	4,710	504	3,270	1,300	197	14.4

[a] CL_{liver}, CL_{urine}, and tissue uptake rate index are expressed as average values for 24 hr after intravenous injection for CMD and 2 hr for Gal-CMD and Man-CMD.

CMD was accumulated in the NPC rather than PC. These findings were in good agreement with those of the glycosylated BSAs.

Competitive Inhibition of Hepatic Uptake Between Glycosylated Dextran and Albumin Derivatives

Table II summarizes the plasma concentration and liver accumulation of glycosylated macromolecules administered with or without the competitors. The uptake of ^{111}In-labeled Gal-BSA by the liver was significantly inhibited by the presence of Gal-CMD, while Man-CMD had no effect. The mannosylated macromolecules competed with each other for the liver uptake and Man-BSA showed a higher inhibitory activity than Man-CMD.

Physicochemical Properties of araC Conjugates

Table III shows the physicochemical properties of araC conjugates with the CMD derivatives. The net charges of conjugates were revealed to be anionic. The numbers of araC molecules attached to the CMD derivatives were almost identical in three conjugates and were 13–16 araC molecules per CMD. In araC-Gal-CMD (II), the numbers of galactose residues were determined to be approximately 140 molecules per CMD. However, the exact number of galactose molecules in araC-Gal-CMD (I) could not be determined by the present method.

araC was gradually released from araC-CMD (Fig. 5), with a half-life of 155 hr at pH 7.0, but the release rate increased with the increase or decrease in buffer pH. araC was also released from ara-C-Gal-CMD (I) with the same rate (half-life = 37 hr) as araC-CMD at pH 7.4.

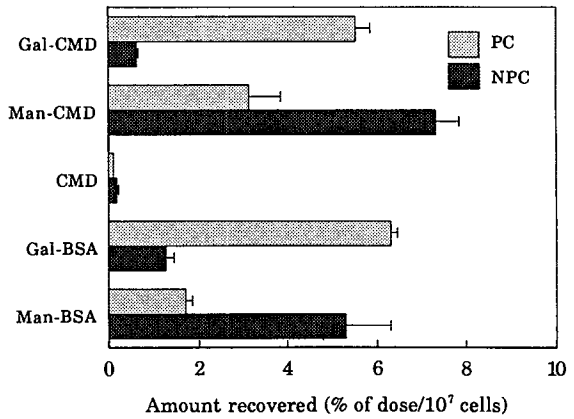

Fig. 4. Cellular localization of ^{14}C-labeled CMD derivatives after intravenous injection in mice at a dose of 1 mg/kg. The distributions of glycosylated BSAs (16) are also shown for comparison. Results are expressed as the mean ± SD of three mice.

In Vivo Disposition Properties of [^{3}H]araC and Its Conjugates with CMD Derivatives

Figure 6 shows the plasma concentration– and liver accumulation–time curves of araC and its conjugates with CMD derivatives after intravenous injection in mice. araC administered in a free form rapidly disappeared from plasma and was excreted into urine. However, araC conjugated to CMD was retained in the blood circulation for a long time and was scarcely accumulated in any tissues including the liver. On the other hand, araC was delivered to the liver, especially to the parenchymal cells, by conjugation to Gal-CMD (data not shown). The rate of liver uptake was quite different for the two kinds of conjugates, and araC-Gal-CMD (II) was taken up by the liver more rapidly than araC-Gal-CMD (I). Table IV summarizes the results of pharmacokinetic analysis. araC had a large urinary clearance but this was drastically decreased by the conjugation to CMD. Hepatic uptake clearance of araC-Gal-CMD (II) was about seven times higher than that of araC-Gal-CMD (I) and rep-

Table II. Competitive Inhibition of Hepatic Uptake of ^{111}In-Labeled Glycosylated Albumins and ^{14}C-Labeled Man-CMD by Other Types of Glycosylated Macromolecule[a]

Compound (time)	Inhibitor	Plasma concentration (% of dose/mL)	Liver accumulation (% of dose)
Gal-BSA	None	0.88 ± 0.27[b]	81.1 ± 3.0
(5 min)	Man-BSA	0.37 ± 0.05	75.2 ± 2.9
	Gal-CMD	35.7 ± 4.30*	33.0 ± 3.1*
	Man-CMD	0.53 ± 0.09	84.0 ± 1.9
Man-BSA	None	6.22 ± 1.01	59.2 ± 2.4
(10 min)	Gal-BSA	8.24 ± 1.50	61.1 ± 2.9
	Man-CMD	27.6 ± 5.40*	43.4 ± 2.7*
Man-CMD	None	3.45 ± 0.54	64.5 ± 4.9
(30 min)	Man-BSA	51.1 ± 3.20*	19.2 ± 5.0*

[a] Radiolabeled compound (1 mg/kg) was injected with inhibitor (10 mg/kg), and plasma concentration and liver accumulation of radiolabeled compound were assayed at the time indicated in parentheses after injection.

[b] Results are expressed as the mean ± SD of three mice.

* Statistically significant difference based on Student's t test ($P < 0.01$) as compared with each control.

Table III. Physicochemical Characteristics of araC Conjugates with Dextran Derivatives

Compounds	Sugar/Dex (mol/mol)	araC/Dex (mol/mol)	Adsorption at pH 7.2 (%) CM-Sephadex	Adsorption at pH 7.2 (%) DEAE-Sephadex
Dextran	—	—	0	0
CMD	—	—	0	98.4
araC-CMD	—	15.8	0	72.9
araC-Gal-CMD (I)	nd[a]	13.9	0	74.1
araC-Gal-CMD (II)	137	12.8	0	74.1

[a] Not determined.

resented the largest part of the total-body clearance. However, uptake rates in other tissues and urinary clearances for the two types of conjugates were similar.

DISCUSSION

Pharmacokinetic analysis was performed assuming that the efflux of the compound from tissues was negligible and uptake clearances were calculated by dividing the amount of radioactivity in the tissue at a sampling time by AUC up to that time. Dextran is known to resist metabolic degradation (23) and ^{14}C-labeled dextran was shown not to suffer degradation in the mouse liver (24). Since a linear relationship was observed between the amount of liver accumulation and the AUC at all sampling times for ^{14}C-labeled Gal-CMD and Man-CMD (data not shown), the above assumption was confirmed to be valid. A similar result was observed also in araC-Gal-CMD (II) (data not shown). Therefore, the results of the pharmacokinetic analysis showed the actual disposition properties of the tested compounds. In a previous investigation (11), we demonstrated that the hepatic uptake of glycosylated BSAs is a nonlinear process and that the calculated uptake clearance represented average values for overall experimental period especially at high doses. However, since the dose of macromolecules was set to 1 mg/kg, where uptake is not saturated, the obtained hepatic clearance value can be considered a direct measure of uptake rate. We compared hepatic uptake and urinary excretion clearances of all tested compounds in Fig. 7 to characterize quantitatively the targeting potential of the conjugates.

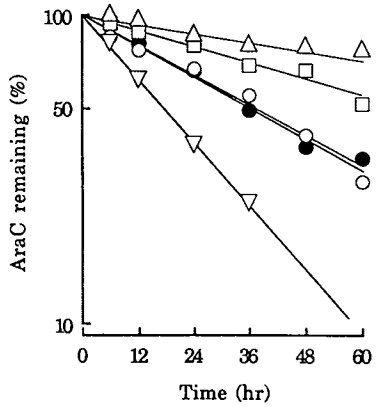

Fig. 5. *In vitro* release of araC from the conjugates with CMD derivatives. Conjugates were incubated in 0.1 *M* phosphate buffer, pH 5.0 (□), pH 7.0 (△), pH 7.4 (○), and pH 8.0 (▽). Open symbols represent araC-CMD and filled symbols represent araC-Gal-CMD.

Dextran seems to be one of the most promising of the macromolecules available as drug carriers (19). However, we have revealed that unmodified dextran is taken up by the liver parenchymal cells due to endocytosis, probably with the asialoglycoprotein receptor (20), and this may disturb specific targeting to the cells besides the hepatocytes. To diminish this undesirable uptake of dextran and to emphasize the efficacy of attached homing devices, we derivatized dextran to a weakly anionized form (CMD). Although dextran sulfate, a strongly anionic form of dextran, is known to be taken up by the scavenger receptors (25), CMD was retained in the circulation for a long period (Fig. 3), indicating little interaction even with the liver sinusoidal cells having the scavenger receptors. Therefore, we used CMD as a very general carrier backbone and attached sugar moieties to CMD to achieve selective delivery to the liver. However, in clinical application, we should further consider the problem of biodegradability (26).

In the present study, the rates and the extents of hepatic uptake of these glycosylated CMDs at 1 mg/kg of dose were shown to be satisfactorily high for selective hepatic targeting. However, hepatic uptake rates of these glycosylated CMDs were somewhat lower than those of glycosylated BSAs, which were almost equal to the hepatic plasma flow rate at doses less than 1 mg/kg (11). The affinity of the glycosylated macromolecules may be determined by the number of incorporated sugar moieties (27,28) as well as the clustering and geometric organization of sugars. However, the number of incorporated sugar moieties in the glycosylated CMDs (approximately 140 sugar moieties per CMD) was higher than that in the glycosylated BSAs (approximately 20 sugar moieties per BSA) and we cannot explain the relationship between the number of sugars and the rate of hepatic uptake from this point of view. The method of glycosylation is also reported to be an important factor for targeting since the attachment of the *p*-aminophenyl derivative of sugar (29,30) increased the negative charge of the conjugates and resulted in uptake by scavenger receptors (31). In Table I, hepatic clearance of Gal-CMD is higher than that of Man-CMD, in accordance with the results of glycosylated BSAs (11). Man-CMD also had a relatively high spleen clearance, probably due to the uptake by macrophages, which recognizes mannose-terminated proteins (32).

In this study, we selected araC as a model drug and tried to deliver it to the liver parenchymal cells utilizing Gal-CMD as a carrier. araC is an antitumor drug used against leukemia (33). Because of its poor permeability to the cell membrane and short half-life due to urinary excretion, the control of the pharmacokinetic properties of araC attracts interest and several studies have been done to enhance the therapeutic efficacy of araC through conjugation to macromolecules (34). We conjugated araC to CMD derivatives via an amide bond (22). We measured the release of araC from the conjugates by absorbance at 272 nm, which represents the free amino group on araC. Therefore, it could be considered that only intact araC, and not the form bound to sugars, was measured by this analytical method. araC was released from the conjugates by hydrolysis by first-order kinetics (Fig. 5), indicat-

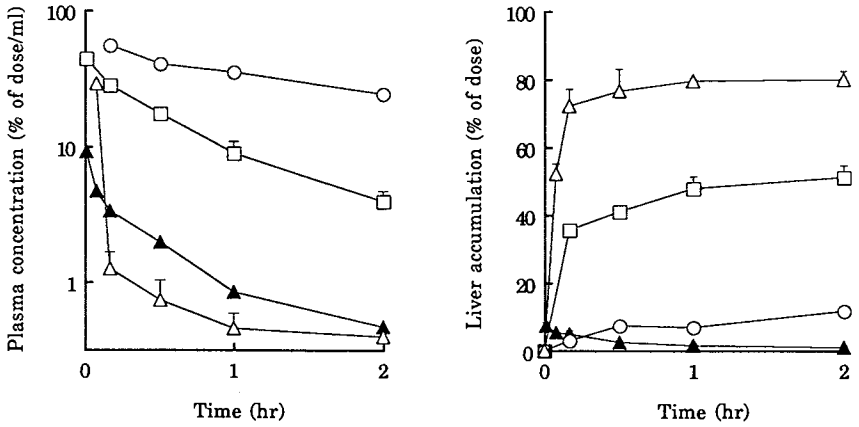

Fig. 6. Plasma concentration- and liver accumulation-time curves of ^{3}H-labeled araC and its conjugates with CMD derivatives after intravenous injection in mice. Results are expressed as the mean ± SD of four mice. (▲) araC; (○) araC-CMD; (□) araC-Gal-CMD (I); (△) araC-Gal-CMD (II).

ing that these conjugates act as macromolecular prodrugs of araC. The release half-life in 0.1 *M* phosphate buffer (pH 7.4) was about 36 hr and the addition of plasma somewhat enhanced the release (half-life = 23 hr). In the present case, the release of araC in plasma might have little effect on the disposition of the araC conjugates since the pharmacokinetic parameters of the conjugates were similar to those of the carriers (Fig. 7). This long half-life of release might result in little efflux of araC from the liver during the experimental period. In order to realize the selective release only in the cells, araC should be bound to macromolecules via an acid-liable or enzymatically cleavable spacer (35,36). The other factor which decreases the efficacy of araC is the rapid metabolism to uracyl β-D-arabinoside (araU) by cytidine deaminase (37), but this should be diminished in the present case since the amino group in araC, an attaching site of deaminase, is blocked by the conjugation. Thus, araC is considered to be stable as long as it is attached to dextran derivatives. In the *in vivo* distribution study, however, araC was determined by the radioactivities and no information on metabolism of araC was obtained.

The *in vivo* behavior of araC was revealed to be destined by the behavior of the carrier macromolecule (Fig. 7) and targeting of araC to the liver was successfully achieved by conjugation to Gal-CMD. However, araC-Gal-CMD (I) synthesized by attaching araC to Gal-CMD showed slower uptake than Gal-CMD or araC-Gal-CMD (II). The physicochemical characteristics of the two conjugates which affect the *in vivo* disposition profiles are similar except for the number of galactose residues (Table III). This suggests that several numbers of the attached galactose residues are detached or denatured during the introduction of araC in araC-Gal-CMD (I), although the final number of available galactose residues could not be directly estimated. Thus the synthetic procedure may ordain the final achievement of drug–carrier conjugate. On the other hand, some drugs are reported to increase the nonspecific interaction with tissues when attached to the carrier backbone (38), but this is not the case in this study.

The changes in numbers of asialoglycoprotein receptors in the liver in a disease state such as cancer are now controversial (39–41). Regardless of this point, the conjugates are expected to exhibit therapeutic activity against, for example, hepatoma cells with some receptors disseminating in the ascitic fluid. We confirmed the receptor-mediated uptake of araC-Gal-CMD (II) in MH134 hepatoma cells (unpublished data).

In this study, we targeted araC to the liver parenchymal cells in three steps, i.e., (1) utilized dextran as a carrier backbone, (2) diminished the nonspecific interaction with tissues by introducing an anionic charge, and (3) utilized a galactose residue as a hepatotropic homing device. This ap-

Table IV. AUC, Clearance, and Tissue Uptake Rate Index for ^{3}H-Labeled araC and Its Conjugates with CMD Derivatives After Intravenous Injection in Mice[a]

Compounds	AUC (% dose hr/mL)	Clearance (μL/hr)			Tissue uptake rate index (μL/hr/g)			
		CL_{total}	CL_{liver}	CL_{urine}	Liver	Spleen	Kidney	Muscle
araC	3.1	28,900	357	23,900	240	503	398	161
araC-CMD	167	596	156	151	130	26.2	22.9	2.0
araC-Gal-CMD (I)	25.5	3,170	2,010	1,150	1,610	177	138	9.5
araC-Gal-CMD (II)	6.6	15,300	13,800	1,310	9,170	83.8	313	101

[a] CL_{liver}, CL_{urine}, and tissue uptake rate index are expressed as average values for 8 hr after intravenous injection for araC-CMD and 2 hr for araC, araC-Gal-CMD (I), and araC-Gal-CMD (II).

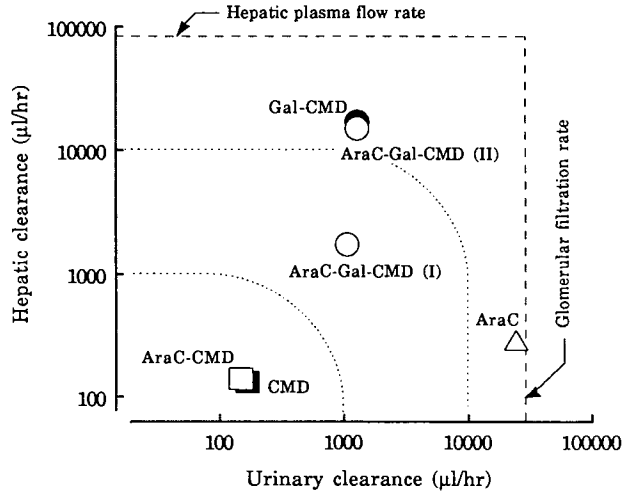

Fig. 7. Hepatic and urinary clearances of ^{14}C-labeled CMD derivatives and ^{3}H-labeled araC conjugates with CMD derivatives in mice.

proach is also applicable to the targeting to the nonparenchymal cells and thus will open a way to therapeutic strategies against various hepatic diseases.

REFERENCES

1. G. Ashwell and A. G. Morell. The role of surface carbohydrates in the hepatic recognition and transport of circulating glycoproteins. *Adv. Enzymol.* 41:99–128 (1974).
2. G. Ashwell and J. Harford. Carbohydrate-specific receptors of the liver. *Annu. Rev. Biochem.* 51:531–554 (1982).
3. R. J. Fallon and A. L. Schwartz. Receptor-mediated delivery of drugs to hepatocytes. *Adv. Drug Deliv. Rev.* 4:49–63 (1989).
4. S. Gordon and S. Rabinowitz. Macrophages as targets for drug delivery. *Adv. Drug Deliv. Rev.* 4:27–47 (1989).
5. D. K. F. Meijer and P. van der Sluijs. Covalent and noncovalent protein binding of drugs: Implications for hepatic clearance, storage, and cell-specific drug delivery. *Pharm. Res.* 6:105–118 (1989).
6. L. Fiume, A. Mattioli, C. Busi, P. G. Balboni, G. Barbanti-Brodano, J. de Vries, R. Altmann, and Th. Wieland. Selective inhibition of ectromelia virus DNA synthesis in hepatocytes by adenine-9-β-D-arabinofuranoside (ara-A) and adenine-9-β-D-arabinofuranoside 5′-monophosphate (ara-AMP) conjugated to asialofetuin. *FEBS Lett.* 116:185–188 (1980).
7. L. Fiume, B. Bassi, C. Busi, A. Mattioli, and G. Spinosa. Drug targeting in antiviral chemotherapy. A chemically stable conjugate of 9-β-D-arabinofuranosyl-adenine 5′-monophosphate with lactosaminated albumin accomplishes a selective delivery of the drug to liver cells. *Biochem. Pharmacol.* 35:967–972 (1986).
8. G. Chaudhuri, A. Mukhopadhyay, and S. K. Basu. Selective delivery of drugs to macrophages through a highly specific receptor. An efficient chemotherapeutic approach against leishmaniasis. *Biochem. Pharmacol.* 38:2995–3002 (1989).
9. L. Fiume, B. Bassi, C. Busi, A. Mattioli, G. Spinosa, and H. Faulstich. Galactosylated poly(L-lysine) as a hepatotropic carrier of 9-β-D-arabinofuranosyladenine 5′-monophosphate. *FEBS Lett.* 203:203–206 (1986).
10. R. Duncan, P. Kopečtová, J. Strohalm, I. C. Hume, J. B. Lloyd, and J. Kopeček. Anticancer agents coupled to N-(2-hydroxypropyl)methacrylamide copolymers. II. Evaluation of daunomycin conjugates in vivo against L1210 leukaemia. *Br. J. Cancer* 57:147–156 (1988).
11. M. Nishikawa, Y. Ohtsubo, J. Ohno, T. Fujita, Y. Koyama, F. Yamashita, M. Hashida, and H. Sezaki. Pharmacokinetics of receptor-mediated hepatic uptake of glycosylated albumin in mice. *Int. J. Pharm.* 85:75–85 (1992).
12. T. Fujita, M. Nishikawa, C. Tamaki, Y. Takakura, M. Hashida, and H. Sezaki. Targeted delivery of human recombinant superoxide dismutase by chemical modification with mono- and polysaccharide derivatives. *J. Pharmacol. Exp. Ther.* 263:971–978 (1992).
13. L. Fiume, C. Busi, P. Preti, and G. Spinosa. Conjugates of ara-AMP with lactosaminated albumin: A study on their immunogenicity in mouse and rat. *Cancer Drug Deliv.* 4:145–150 (1987).
14. M. Hashida, A. Kato, Y. Takakura, and H. Sezaki. Disposition and pharmacokinetics of a polymeric prodrug of mitomycin C, mitomycin C-dextran conjugate, in the rat. *Drug Metab. Dispos.* 12:482–499 (1984).
15. Y. Takakura, A. Takagi, M. Hashida, and H. Sezaki. Disposition and tumor localization of mitomycin C-dextran conjugates in mice. *Pharm. Res.* 4:293–300 (1987).
16. Y. Takakura, R. Atsumi, M. Hashida, and H. Sezaki. Development of a novel polymeric prodrug of mitomycin C, mitomycin C-dextran conjugate with anionic charge. II. Disposition and pharmacokinetics following intravenous and intramuscular administration. *Int. J. Pharm.* 37:145–154 (1987).
17. H. Sezaki, Y. Takakura, and M. Hashida. Soluble macromolecular carriers for the delivery of antitumour drugs. *Adv. Drug Deliv. Rev.* 3:247–266 (1989).
18. Y. Takakura, T. Fujita, M. Hashida, and H. Sezaki. Disposition characteristics of macromolecules in tumor-bearing mice. *Pharm. Res.* 7:339–346 (1990).
19. C. Larsen. Dextran prodrugs—structure and stability in relation to therapeutic activity. *Adv. Drug Deliv. Rev.* 3:103–154 (1989).
20. M. Nishikawa, F. Yamashita, Y. Takakura, M. Hashida, and H. Sezaki. Demonstration of receptor-mediated hepatic uptake of dextran in mice. *J. Pharm. Pharmacol.* 44:396–401 (1992).
21. Y. C. Lee, C. P. Stowell, and M. K. Krantz. 2-imino-2-methoxyethyl 1-thioglycosides: New reagents for attaching sugars to proteins. *Biochemistry* 15:3956–3963 (1976).
22. P. D. G. Dean, P. H. Rowe, and D. Exley. Preparation of 6-oxoestriol-6-[O-(carboxymethyl)-oxime] and 6-oxoestrone 6-[O-(carboxymethyl)oxime]–bovine serum albumin conjugates. *Steroids Lipids Res.* 3:82–89 (1972).
23. R. W. Mowry and C. M. Millican. A histochemical study of the distribution and fate of dextran in tissues of the mouse. *Am. J. Pathol.* 29:523–540 (1953).
24. R. G. Melton, C. N. Wiblin, A. Baskerville, R. L. Foster, and R. F. Sherwood. Covalent linkage of carboxypeptidase G_2 to soluble dextrans. II. In vivo distribution and fate of conjugates. *Biochem. Pharmacol.* 36:113–121 (1987).
25. M. S. Brown, S. K. Basu, J. R. Falck, Y. K. Ho, and J. L. Goldstein. The scavenger cell pathway for lipoprotein degradation: Specificity of the binding site that mediates the uptake of negatively-charged LDL by macrophages. *J. Supramol. Struct.* 13:67–81 (1980).
26. J. Drobník. Biodegradable soluble macromolecules as drug carriers. *Adv. Drug Deliv. Rev.* 3:229–245 (1989).
27. P. H. Schlesinger, J. S. Rodman, T. W. Doebber, P. D. Stahl, Y. C. Lee, C. P. Stowell, and T. B. Kuhlenschmidt. The role of extra-hepatic tissues in the receptor-mediated plasma clearance of glycoproteins terminated by mannose or N-acetylglucosamine. *Biochem. J.* 192:597–606 (1980).
28. D. R. Vera, K. A. Krohn, R. C. Stadalnik, and P. O. Scheibe. Tc-99m galactosyl-neoglycoalbumin: In vitro characterization of receptor-mediated binding. *J. Nucl. Med.* 25:779–787 (1984).
29. C. R. McBroom, C. H. Colleen, H. Samanen, and I. J. Goldstein. Carbohydrate antigens: Coupling of carbohydrates to proteins by diazonium and phenylisothiocyanate reactions. *Methods Enzymol.* 28:212–219 (1972).
30. M. Monsigny, C. Kieda, and A. C. Roche. Membrane glycoproteins glycolipids and membrane lectins as recognition signals in normal and malignant cells. *Biol. Cell* 47:95–110 (1983).
31. R. W. Jansen, G. Molema, T. L. Ching, R. Oosting, G. Harms, F. Moolenaar, M. J. Hardonk, and D. K. F. Meijer. Hepatic endocytosis of varous types of mannose-terminated albumins. What is important, sugar recognition, net charge, or the combination of these features. *J. Biol. Chem.* 266:3343–3348 (1991).
32. J. A. Summerfield, J. Vergalla, and E. A. Jones. Modulation of a glycoprotein recognition system on rat hepatic endothelial

cells by glucose and diabetes mellitus. *J. Clin. Invest.* 69:1337–1347 (1982).
33. D. H. W. Ho and E. Frei. Clinical pharmacology of 1-β-D-arabinofuranosyl cytosine. *Clin. Pharmacol. Ther.* 12:944–954 (1971).
34. Y. Kato, M. Saito, H. Fukushima, Y. Takeda, and T. Hara. Antitumor activity of 1-β-D-arabinofuranosylcytosine conjugated with polyglutamic acid and its derivative. *Cancer Res.* 44:25–30 (1984).
35. W. C. Shen and H. J. P. Ryser. Cis-aconityl spacer between daunomycin and macromolecular carriers: A model of pH-sensitive linkage releasing drug from a lysosomotropic conjugate. *Biochem. Biophys. Res. Commun.* 102:1048–1054 (1981).
36. A. Trouet, M. Masquelier, R. Baurain, and D. D. D. Campeneere. A covalent linkage between daunorubicin and proteins that is stable in serum and reversible by lysosomal hydrolases, as required for a lysosomotropic drug-carrier conjugate: In vitro and in vivo studies. *Proc. Natl. Acad. Sci. USA* 79:626–629 (1982).
37. G. W. Camiener and C. G. Smith. Studies of the enzymatic deamination of cytosine arabinoside. I. Enzymatic distribution and species specificity. *Biochem. Pharmacol.* 14:1405–1416 (1965).
38. R. Duncan, H. C. Cable, P. Rejmanová, J. Kopeček, and J. B. Lloyd. Tryosinamide residues enhance pinocytic capture of N-(2-hydroxypropyl)methacrylamide copolymers. *Biochim. Biophys. Acta* 799:1–8 (1984).
39. T. Sawamura, H. Nakada, H. Hazama, Y. Shiozaki, Y. Sameshima, and Y. Tashiro. Hyperasialoglycoproteinemia in patients with chronic liver diseases and/or liver cell carcinoma. *Gastroenterology* 87:1217–1221 (1984).
40. Y. J. Schneider, J. Abarca, E. Aboud-Pirak, R. Baurain, F. Ceulemans, D. Deprez-De Campeneere, B. Lesur, M. Masquelier, C. Otte-Slachmuylder, D. Rolin-van Swieten, and A. Trouet. Drug targeting in human cancer chemotherapy. In G. Gregoriadis, G. Poste, J. Senior, and A. Trouet, (eds.), *Receptor-Mediated Targeting of Drugs*, NATO ASI Series A, Life Sciences Vol. 82, Plenum Press, New York, 1984, pp. 1–25.
41. C. Eisenberg, N. Seta, M. Appel, G. Feldman, G. Durand, and J. Feger. Asialoglycoprotein receptor in human isolated hepatocytes from normal liver and its apparent increase in liver with histological alterations. *J. Hepatol.* 13:305–309 (1991).